

Stabilization of Plutonium Nano-Colloids by Epitaxial Distortion on Mineral Surfaces

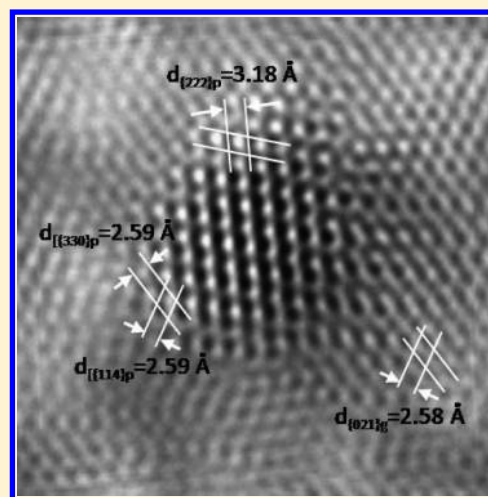
Brian A. Powell,^{*,†} Zurong Dai,[‡] Mavrik Zavarin,[‡] Pihong Zhao,[‡] and Annie B. Kersting[‡]

[†]Environmental Engineering and Earth Sciences, Clemson University, 342 Computer Court, Anderson, South Carolina 29625, United States

[‡]Glenn T. Seaborg Institute, Physical and Life Sciences Directorate, Lawrence Livermore National Laboratory, 7000 East Avenue, Livermore, California 94550, United States

S Supporting Information

ABSTRACT: The subsurface migration of Pu may be enhanced by the presence of colloidal forms of Pu. Therefore, complete evaluation of the risk posed by subsurface Pu contamination needs to include a detailed physical/chemical understanding of Pu colloid formation and interactions of Pu colloids with environmentally relevant solid phases. Transmission electron microscopy (TEM) was used to characterize Pu nanocolloids and interactions of Pu nanocolloids with goethite and quartz. We report that intrinsic Pu nanocolloids generated in the absence of goethite or quartz were 2–5 nm in diameter, and both electron diffraction analysis and HRTEM confirm the expected $Fm\bar{3}m$ space group with the fcc, PuO_2 structure. Plutonium nanocolloids formed on goethite have undergone a lattice distortion relative to the ideal fluorite-type structure, fcc, PuO_2 , resulting in the formation of a bcc, Pu_4O_7 structure. This structural distortion results from an epitaxial growth of the plutonium colloid on goethite, leading to stronger binding of plutonium to goethite compared with other minerals such as quartz, where the distortion was not observed. This finding provides new insight for understanding how molecular-scale behavior at the mineral–water interface may facilitate transport of plutonium at the field scale.



INTRODUCTION

It has been recently recognized that plutonium, once thought immobile in the subsurface, can be transported with the colloidal fraction of groundwater.^{1–3} Despite this paradigm shift, a comprehensive understanding of the biogeochemical mechanisms controlling plutonium migration remains elusive and hinders progress on the development of reliable contaminant transport models. In a field study at the Nevada Test Site, Kersting et al.¹ documented the unexpected appearance of Pu down-gradient from its known source, contradicting the conventional view of Pu immobility in groundwater by showing that colloids facilitated the transport of Pu. Although not a new idea,^{4,5} colloid-facilitated transport has slowly gained acceptance and was further supported by recent studies of Novikov et al.² and Xu et al.³ showing that Pu transported from its source was adsorbed to iron hydroxides and organic colloids, respectively. Nevertheless, fundamental details of the physical and chemical mechanisms that control this process are not well understood and continue to hinder both theoretical and modeling advances.

Plutonium (Pu), a highly toxic, long-lived radionuclide, has very complex chemical and physical properties, and much attention has been paid to understanding its behavior in order

to guarantee safe handling and long-term storage. The potential for environmental transport of Pu and other radionuclides is a contentious issue for the disposal of nuclear waste and remains a major impediment to the further development of nuclear energy. During the U.S. nuclear weapons program, approximately 12000 Ci of Pu-239 was discharged into the subsurface at the Hanford Nuclear Reservation,⁶ and approximately 2775 kg (8.3×10^5 Ci) of Pu was deposited underground at the Nevada Test Site as a result of underground nuclear testing.⁷ In addition, the Yucca Mountain Repository was designed to store 645 MT of Pu.⁸ These subsurface inventories coupled with a long half-life (i.e., Pu-239 $t_{1/2} = 24,100$ yrs) mean that Pu will remain in our environment for an extremely long time. The inability to safely treat, contain, or dispose of Pu and other actinides presents a serious scientific challenge.

Current contaminant transport models do not reliably predict the subsurface behavior of many radionuclides because our

Received: October 2, 2010

Accepted: January 18, 2011

Revised: January 7, 2011

Published: February 28, 2011

understanding of their behavior at the molecular level is insufficient to develop macroscopic thermodynamic models for their chemistry.⁹ Several recent studies have continued to expand our understanding of Pu chemistry. For example, detailed thermodynamic analysis of plutonium speciation has demonstrated a complex chemistry with plutonium capable of existing in multiple oxidation states and forming numerous solid phases.^{10,11} Of particular note was the description of a colloidal Pu(IV) phase that is in equilibrium with several aqueous Pu oxidation states as well as solid phases.¹¹ Soderholm et al.,¹² identified Pu nanoclusters of $[\text{Pu}_{38}\text{O}_{56}\text{Cl}_{54}(\text{H}_2\text{O})_8]^{14-}$, which can aggregate to form colloids of the size range of those presented in this work. Incorporation of this molecular level understanding of Pu speciation is necessary to properly constrain reactive transport models. Thus, a current challenge is to explore the molecular-scale behavior of contaminants at the mineral–water interface for development of macroscopic models.

The chemical behavior of Pu (i.e., aqueous speciation, solubility, sorptivity, redox chemistry, and affinity for colloidal particles) is particularly complex.¹³ Pu can exist in as many as four oxidation states at environmentally relevant solutions conditions (+3, +4, +5, or +6), and kinetics of redox equilibrium are often slow under environmental conditions. The solubility and sorptivity of different oxidation states vary dramatically.¹⁴ Under most soil conditions, Pu is predominantly in the tetravalent state,¹⁴ and many studies have shown that soluble Pu(V) reduces to the more insoluble Pu(IV) on the surface of goethite and other minerals and sediments.^{15–19} Plutonium is highly reactive and can both attach to naturally occurring colloids or hydrolyze becoming its own colloid (sometimes referred to as an “intrinsic” colloid).²⁰ Colloids, defined as $<1\ \mu\text{m}$ particles, have both natural and anthropogenic origins in groundwater. They are transported by groundwater flow and can be composed of inorganic material, organic material, or microorganisms.

In this study, we examined the nanostructure of Pu(IV) colloids on two common minerals, quartz ($\alpha\text{-SiO}_2$) and goethite ($\alpha\text{-FeOOH}$). The challenge of characterizing the structure and chemistry of Pu nanocolloids was accomplished by employing a number of transmission electron microscopy (TEM) techniques, including selected-area electron diffraction, X-ray energy dispersive spectroscopy (EDS), high angle annular dark-field (HAADF) detector STEM imaging, and high-resolution TEM imaging (HRTEM) combined with fast Fourier transform (FFT) analysis. We combined HAADF Z contrast STEM imaging with X-ray EDS to create a powerful technique for identifying nanometer-scale, high atomic mass particles at very low abundances.

MATERIALS AND METHODS

Preparation of Pu Working Solution. A Pu working solution was prepared from a mixed isotope ^{238}Pu , ^{239}Pu , and ^{242}Pu stock solution with activity fractions of 20.2%, 4.8%, and 75%, respectively. The stock solution was purified using BioRad $1 \times 8\ \text{AG}\ 100\text{--}200$ mesh resin and loaded on the resin in 7.5 M HNO_3 , washed with 3 column volumes of 7.5 M HNO_3 , and then eluted in 0.1 M HCl. The final concentration of Pu in the purified stock solution was determined (1) radioanalytically via ^{238}Pu and ^{239}Pu alpha counting on a Packard TR2900 alpha/beta discrimination liquid scintillation counter (LSC) and (2) by mass spectrometry with a Thermo X Series II inductively coupled plasma mass spectrometer (ICP-MS). Although the oxidation state of Pu in the solution was not determined explicitly, successful separation using the above proce-

dures requires Pu(IV). The final concentration of the Pu(IV) working solution was $7\ \mu\text{M}$.

Preparation of Intrinsic Pu Colloids. Intrinsic Pu colloids were prepared by diluting the Pu working solution to $1.0 \times 10^{-6}\ \text{M}$, then raising the pH to 7 with NaOH. The solution containing Pu colloids was passed through a 3k MWCO filter (Pall, Microsep) to retain the colloids on the filter. The colloids were removed from the filter by adding distilled water to the filter reservoir and sonicating the filter apparatus. The sonicated solution was removed and diluted in DDI H_2O . A $5\ \mu\text{L}$ aliquot was transferred to a carbon coated Cu grid for TEM analysis.

Pu Interactions with Quartz and Goethite. Quartz particles were prepared from high purity quartz sand. Goethite particles were synthesized from $\text{Fe}(\text{NO}_3)_3 \cdot 9\text{H}_2\text{O}$ as described by Schwertmann and Cornell²¹ (see the Supporting Information for additional details of quartz and goethite synthesis and characterization). Plutonium was added to goethite and quartz in two different ways (see the Supporting Information for additional details). In the first experiment, an aliquot of intrinsic Pu(IV) nanocolloids in solution was added to the goethite mineral suspension, agitated for one week, centrifuged, and separated. The final concentration of Pu(IV) in the intrinsic Pu nanocolloid suspension was $0.9\ \mu\text{M}$. In the second experiment, small volumes of soluble Pu(IV) stock solution were added incrementally to goethite and quartz suspensions (Table S1 of the Supporting Information). The final concentrations of Pu(IV) in the quartz and goethite solutions were 3.87 and $0.99\ \mu\text{M}$, respectively. The partitioning of the Pu nanocolloids between the aqueous phase and the mineral phase was monitored using liquid scintillation counting. The nanostructure of Pu colloids was investigated using HRTEM for four different samples: (1) intrinsic Pu nanocolloids, (2) intrinsic Pu nanocolloids added to goethite colloids, (3) soluble Pu(IV) added incrementally to goethite colloids, and (4) soluble Pu(IV) added incrementally to quartz colloids.

RESULTS AND DISCUSSION

Intrinsic Pu nanocolloids were 2–5 nm in diameter, and both electron diffraction analysis and HRTEM analysis confirm the expected fcc PuO_2 crystal structure with $Fm\bar{3}m$ space group (Figure 1 and Table S2 of the Supporting Information). The intrinsic Pu nanocolloids were similar in both appearance and size to those previously observed²² and were recently reported by Soderholm et al.,¹² suggesting that the commonly described Pu “polymer” is instead an aggregated mass of nanosized Pu clusters and/or colloids. Recent extended X-ray absorption fine structure (EXAFS) studies have identified oxidation of bulk PuO_2 to PuO_{2+x} . Oxidation of PuO_2 results in formation of axial $\text{O}=\text{Pu}=\text{O}$ bonds with lengths $<1.9\ \text{\AA}$ and a structural distortion of the PuO_2 phase.^{23,24} Similar oxidative distortion was not observed in the PuO_2 nanocolloids in this study and was not reported in other recent studies.^{12,25}

In the experiment in which intrinsic Pu nanocolloids were formed first and then mixed with goethite colloids, the majority of the Pu nanocolloids did not associate with goethite and instead remained as nanocolloids captured on the carbon support film of the TEM grid (Figure 2A). HRTEM imaging (Figure 2B) and FFT analysis (Figure 2E–F) of the intrinsic Pu nanocolloids found on the carbon grid, and the few associated with the goethite (box in Figure 2B), retained the same fcc PuO_2 structure as the original

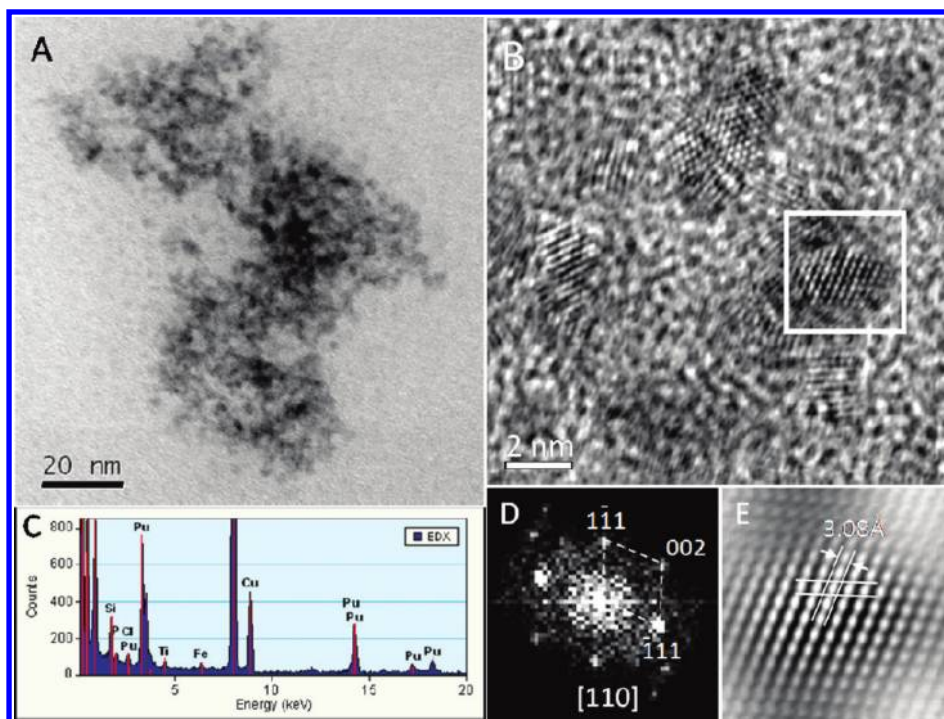


Figure 1. Intrinsic Pu nanocolloids on carbon film. (A) Low-magnification brightfield TEM image of a cluster of intrinsic Pu nanocolloids. (B) HRTEM image. (C) EDX spectrum of Pu nanocolloids in panel (A). (D) FFT of individual Pu nanocolloid from box in panel (B), showing the fcc, PuO₂ structure. (E) Filtered image of the Pu colloid in the box in panel (B), showing a lattice image of fcc, PuO₂, nanocolloid. Electron beam is parallel to the [110] zone.

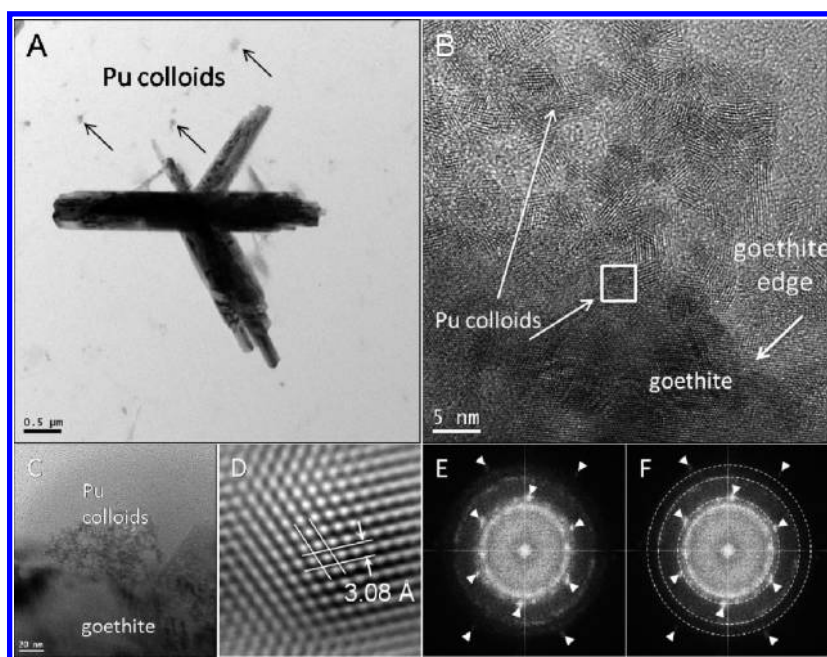


Figure 2. Intrinsic PuO₂ nanocolloids and goethite. (A) Low-magnification TEM image showing large tabular crystals of goethite and intrinsic Pu nanocolloids. (B) HRTEM image of Pu nanocolloids on goethite and near the edge of goethite. (C) Brightfield TEM image showing Pu nanocolloids located at edge of goethite grain. (D) HRTEM image of an individual PuO₂ nanocolloid on goethite, marked by white box in panel (B). (E,F) FFT of HRTEM image shown in panel (B), in which the reflections indicated by arrowheads are from goethite, and reflections located on rings are the fcc, PuO₂.

intrinsic Pu nanocolloids (Tables S3 and S4 of the Supporting Information).

In contrast, Pu nanocolloids formed by incrementally adding a soluble Pu(IV) solution to a goethite suspension formed 2–5 nm nanocolloids on the mineral surface (Figure 3A). HRTEM

imaging and electron diffraction analysis show that these nanocolloids do not have the expected *Fm3m* space group but rather the *Ia3* space group, matching the bcc Pu₄O₇ crystal structure (Figure 3B–F). Some of the diffraction features are relatively weak in this system due to the limited population of Pu nanocolloids and the challenge of

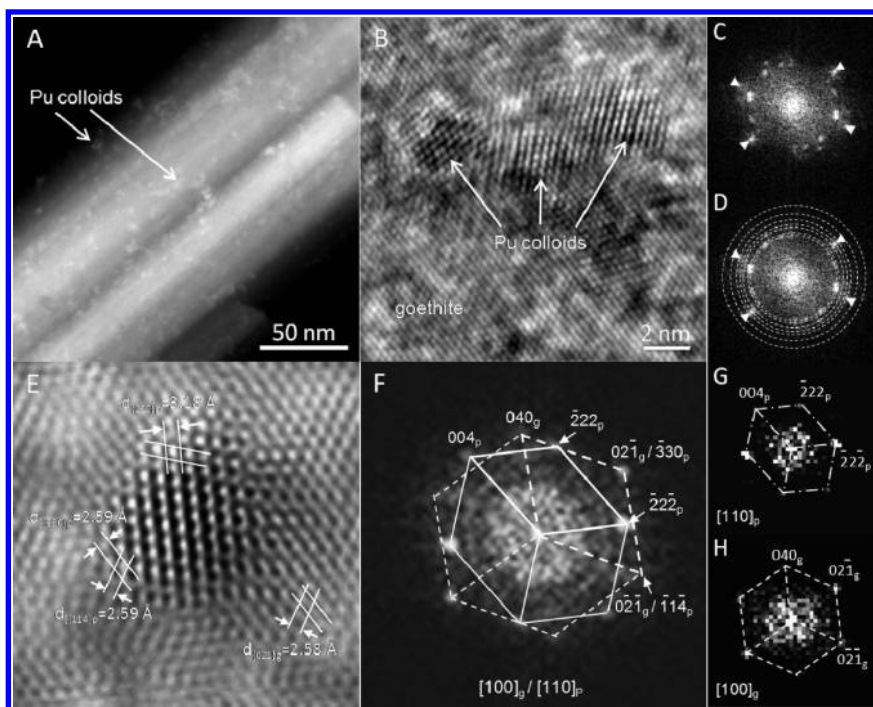


Figure 3. Pu nanocolloids formed in situ on goethite. (A) HAADF STEM image showing Pu nanocolloids (with highly bright contrast) growing on goethite. (B) HRTEM image of Pu_4O_7 nanocolloids on goethite. (C,D) FFT of the HRTEM image shown in panel (B), in which the reflections indicated by arrowheads are from goethite, and reflections located on rings are the bcc, Pu_4O_7 structure. (E) HRTEM image of an individual Pu_4O_7 nanoparticle on goethite, showing the lattice orientation relationship between Pu_4O_7 and goethite. Lighter background is the host goethite, and the darker image is the single Pu colloid. Lower case g and p next to the d -spacing denotes the phase goethite and Pu nanocolloid, respectively. There is a periodic relationship at 2.59 Å between the host goethite {021} and the Pu {114} or Pu {330} crystal plane. (F) FFT of the HRTEM image shown in panel (E), showing the orientation relationship between the two phases. (G,H) FFT of the Pu_4O_7 colloid and FFT of goethite, respectively, from panel (E).

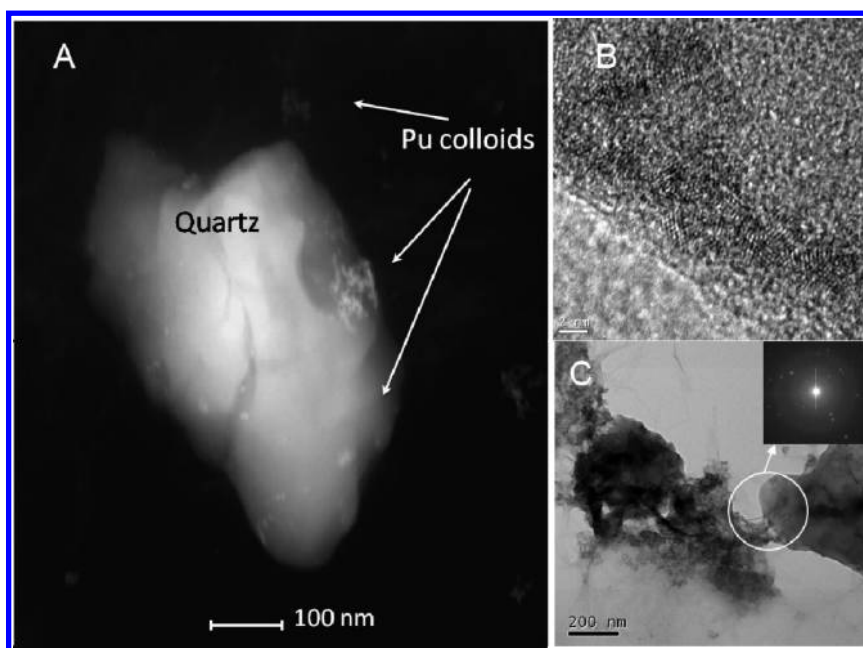


Figure 4. Pu nanocolloids on quartz. (A) HAADF STEM image of Pu nanocolloids on quartz. (B) HRTEM image. (C) Select area electron diffraction analysis indicates the Pu nanocolloids have the fcc, PuO_2 structure.

imaging 2–5 nm nanocolloids. Therefore, the observation of the bcc Pu_4O_7 structure was verified on over 100 Pu nanocolloids using these same techniques (Table S5 of the Supporting Information). Figure S2 of the Supporting Information compares the

FFT of HRTEM images of Pu nanocolloids on goethite against model reflections and fitted rings for PuO_2 and Pu_4O_7 . It is noteworthy that the model structure for hypothetical Pu_4O_9 as described by Petit et al.²⁶ does not match the

Table 1. Summary of *d*-Spacings Observed for Pu Nano-Colloids

sample ID	no. of colloids	<i>d</i> ₁ (Å)	<i>d</i> ₂ (Å)	<i>d</i> ₃ (Å)
PuO ₂ / <i>Fm3m</i>		3.08	2.67	1.89
intrinsic colloids	317	3.08 (0.01)	2.66 (0.03)	1.82 (0.03)
intrinsic Pu nanocolloids on goethite	74	3.09 (0.01)	2.69 (0.01)	1.89 (0.01)
quartz	118	3.08 (0.02)	2.68 (0.02)	1.9 (0.02)
Pu nanocolloids grown on goethite	99	3.19 (0.02)	2.96 (0.05)	2.73 (0.02)
Pu ₄ O ₇ / <i>Ia3</i>		3.18	2.95	2.76

distorted structure of Pu nanocolloids observed in this study (Figure S3 of the Supporting Information).

A strong association of Pu nanocolloids with the goethite surface is shown by an epitaxial relationship between the two phases. The similar *d*-spacing (~2.59 Å) measured between goethite {021} and Pu₄O₇ {114} and {330} crystal planes (Figure 3B–G) allows structural alignment of the two phases. Structurally, the bcc Pu₄O₇ has a distorted fluorite structure and contains oxygen vacancies. It can be considered a superstructure of the ideal fcc fluorite PuO₂, of which structural unit consists of eight unit cells of the fluorite PuO₂.

The plutonium nanocolloids formed by sorbing soluble Pu(IV) incrementally on quartz are shown in Figure 4. Small nanocolloids of Pu oxide on quartz formed similar in size to those formed on goethite. However, in this case, the Pu nanocolloids on the quartz have the same structure as intrinsic nanocolloids, fcc, PuO₂ (Figure 4 and Table S6 of the Supporting Information). The lack of a lattice match in this case appears to preclude the epitaxial relationship seen with goethite.

Table 1 provides a summary of the different *d*-spacings observed for all nanocolloids analyzed in this work. The influence of the epitaxial relationship of Pu nanocolloids with goethite can be seen by the similarity in the *d*-spacings of Pu₄O₇ and the Pu nanocolloids which were “grown” incrementally by adding soluble Pu to a goethite suspension. Experiments indicate Pu has a higher sorption affinity for iron (oxyhydr)oxides than silicates.^{27–29} This may be because the possibility of forming an epitaxial relationship results in a stronger attachment to goethite compared to quartz. The fact that Fe(III) and Pu(IV) have similar charge-to-ionic-radius ratios may also play a role in the strong binding of both Pu nanocolloids and Pu ions to iron oxide surfaces. Observed lower desorption rates of Pu from goethite compared to silicates may be due to the epitaxial relationship developed as the Pu is deposited on the goethite.³⁰ In addition, a lower desorption rates of Pu nanocolloids to minerals like goethite may explain the ability of these mineral colloids to transport Pu on the field-scale as observed by Kersting et al.¹ and Novikov et al.²

It is commonly assumed that the aqueous concentration of Pu in natural waters is controlled by sparingly soluble Pu hydrous oxide.^{10,11} The aqueous chemistry of Pu has been described by Neck et al.,¹⁰ as an equilibrium between dissolved oxidation states of Pu, colloidal Pu(IV), and a PuO_{2+x} precipitate. The Pu bulk phases have been characterized as a PuO_{2+x} moiety.²⁴ The formation of Pu₄O₇ nanocolloids on the Fe-bearing, goethite surfaces may limit formation of an oxidized PuO_{2+x} phase, instead resulting in partial reduction relative to PuO₂. These are the first observations that Pu nanocolloids form a distorted fluorite structure of bcc, Pu₄O₇ as a result of epitaxial growth on goethite. This structural distortion is indicative of a strong bond of the Pu nanocolloid to goethite. This stronger bonding has implications to our conceptual

understanding of colloid facilitated Pu transport as Pu could be more strongly bonded to iron oxide natural colloids than other minerals or transported as a free Pu nanocolloid. Although this study investigated the interaction of Pu colloids on inorganic minerals at a given pH, the impact of changing groundwater conditions, the presence of dissolve organic matter, microbial activity, and variable Pu concentrations will also play, as yet undetermined, a role in governing the transport of Pu in the subsurface. This work has demonstrated that the application of nanoscience techniques can provide an important window onto molecular-scale processes at the water–mineral interface that have implications for processes occurring on the kilometer scale.

■ ASSOCIATED CONTENT

S Supporting Information. Detailed discussion of materials and methods, tables of *d*-spacings of examined Pu nanocolloids, sorption isotherm of Pu sorption to goethite from incremental additions, and model compound calculations of PuO₂, Pu₄O₇, and Pu₄O₉. This material is available free of charge via the Internet at <http://pubs.acs.org>.

■ AUTHOR INFORMATION

Corresponding Author

*E-mail: bpowell@clermson.edu; phone: (864) 656-1004; fax: (864) 656-0672.

■ ACKNOWLEDGMENT

Prepared by LLNL under Contract DE-AC52-07NA27344. This work was supported by the Subsurface Biogeochemical Research Program of the U.S. Department of Energy’s Office of Biological and Environmental Research.

■ REFERENCES

- (1) Kersting, A. B.; Efurud, D. W.; Finnegan, D. L.; Rokop, D. J.; Smith, D. K.; Thompson, J. L. Migration of plutonium in ground water at the Nevada Test Site. *Nature* **1999**, *397*, 56.
- (2) Novikov, A. P.; Kalmykov, S. N.; Utsunomiya, S.; Ewing, R. C.; Horreard, F.; Merkulov, A.; Clark, S. B.; Tkachev, V. V.; Myasoedov, B. F. Colloid transport of plutonium in the far-field of the Mayak Production Association, Russia. *Science* **2006**, *314*, 638.
- (3) Xu, C.; Santschi, P. H.; Zhong, J. Y.; Hatcher, P. G.; Francis, A. J.; Dodge, C. J.; A., R. K.; Hung, C. C.; Honeyman, B. D. Colloidal cutin-like substances cross-linked to siderophore decomposition products mobilizing plutonium from contaminated soils. *Environ. Sci. Technol.* **2008**, *42*, 211.
- (4) McCarthy, J.; Zachara, J. ES&T Features: Subsurface transport of contaminants. *Environ. Sci. Technol.* **1989**, *23*, 496.
- (5) Kim, J. I.; Zeh, P.; Delakowitz, B. Chemical interactions of actinide ions with groundwater colloids in Gorleben aquifer systems. *Radiochim. Acta* **1992**, *58–9*, 147.

- (6) Cantrell, K. J. *Transuranic Contamination in Sediment and Groundwater at the U.S. DOE Hanford Site*; Technical Report PNNL-18640; Pacific Northwest National Laboratory, Richland, WA, 2006.
- (7) Smith, D. K.; Finnegan, D. L.; Bowen, S. M. An inventory of long-lived radionuclides residual from underground nuclear testing at the Nevada Test Site, 1951–1992. *J. Environ. Radio.* **2003**, *67*, 35.
- (8) *Yucca Mountain Repository: Safety Analysis Report*; Report DOE/RW-0573, Rev. 1, Draft A; U.S. Department of Energy: Washington, DC, 2009.
- (9) *Basic Research Needs for Geosciences: Facilitating 21st Century Energy Systems*; Report from the Workshop Held February 21–23, 2007; Office of Basic Energy Sciences, U.S. Department of Energy: Bethesda, MD, 2007; p 186.
- (10) Neck, V.; Altmaier, M.; Seibert, A.; Yun, J. I.; Marquardt, C. M.; Fanghanel, T. Solubility and redox reactions of Pu(IV) hydrous oxide: Evidence for the formation of $\text{PuO}_{2+x}(\text{s, hyd})$. *Radiochim. Acta* **2007**, *95*, 193.
- (11) Neck, V.; Kim, J. I. Solubility and hydrolysis of tetravalent actinides. *Radiochim. Acta* **2001**, *89*, 1.
- (12) Soderholm, L.; Almond, P. M.; Skanthakumar, S.; Wilson, R. E.; Burns, P. C. The structure of the plutonium oxide nanocluster $[\text{Pu}_{38}\text{O}_{56}\text{Cl}_{54}(\text{H}_2\text{O})(8)]^{14-}$. *Angew. Chem.-Int. Edit.* **2008**, *47*, 298.
- (13) Silva, R. J.; Nitsche, H. Actinide environmental chemistry. *Radiochim. Acta* **1995**, *70–1*, 377.
- (14) Choppin, G. R. Solution chemistry of the actinides. *Radiochim. Acta* **1983**, *32*, 43.
- (15) Keeney-Kennicutt, W. L.; Morse, J. W. The redox chemistry of Pu(V)O_2^+ interaction with common mineral surfaces in dilute solutions and seawater. *Geochim. Cosmochim. Acta* **1985**, *49*, 2577.
- (16) Shaughnessy, D. A.; Nitsche, H.; Booth, C. H.; Shuh, D. K.; Waychunas, G. A.; Wilson, R. E.; Gill, H.; Cantrell, K. J.; Serme, R. J. Molecular interfacial reactions between Pu(VI) and manganese oxide minerals manganite and hausmannite. *Environ. Sci. Technol.* **2003**, *37*, 3367.
- (17) Powell, B. A.; Fjeld, R. A.; Kaplan, D. I.; Coates, J. T.; Serkiz, S. M. Pu(V)O₂⁺ adsorption and reduction by synthetic hematite and goethite. *Environ. Sci. Technol.* **2005**, *39*, 2107.
- (18) Kaplan, D. I.; Powell, B. A.; Demirkanli, D. I.; Fjeld, R. A.; Molz, F. J.; Serkiz, S. M.; Coates, J. T. Influence of oxidation states on plutonium mobility during long-term transport through an unsaturated subsurface environment. *Environ. Sci. Technol.* **2004**, *38*, 5053.
- (19) Kalmykov, S. N.; Kriventsov, V. V.; Teterin, Y. A.; Novikov, A. P. Plutonium and neptunium speciation bound to hydrous ferric oxide colloids. *C. R. Chim.* **2007**, *10*, 1060.
- (20) Kim, J. I. In *Handbook on the Physics of the Actinides*; Freeman, A. J., Keller, C., Eds.; Elsevier Science Publishers B: Amsterdam, 1986; Vol. 8, p 413.
- (21) Schwertmann, U.; Cornell, R. M. *Iron Oxidies in the Laboratory: Preparation and Characterization*; VCH Publishers, Inc.: New York, 1991.
- (22) Haire, R. G.; Lloyd, M. H.; Beasley, M. L.; Milligan, W. O. Aging of hydrous plutonium dioxide. *J. Electron Microsc.* **1971**, *20*, 8.
- (23) Haschke, J. M.; Allen, T. H.; Morales, L. A. Reaction of plutonium dioxide with water: Formation and properties of PuO_{2+x} . *Science* **2000**, *287*, 285.
- (24) Conradson, S. D.; Begg, B. D.; Clark, D. L.; den Auwer, C.; Ding, M.; Dorhout, P. K.; Espinosa-Faller, F. J.; Gordon, P. L.; Haire, R. G.; Hess, N. J.; Hess, R. F.; Keogh, D. W.; Morales, L. A.; Neu, M. P.; Paviet-Hartmann, P.; Runde, W.; Tait, C. D.; Veirs, D. K.; Villella, P. M. Local and nanoscale structure and speciation in the $\text{PuO}_{2+x-y}(\text{OH})_{2y} \cdot z\text{H}_2\text{O}$ system. *J. Am. Chem. Soc.* **2004**, *126*, 13443.
- (25) Rothe, J.; Walther, C.; Denecke, M. A.; Fanghanel, T. XAFS and LIBD investigation of the formation and structure of colloidal Pu(IV) hydrolysis products. *Inorg. Chem.* **2004**, *43*, 4708.
- (26) Petit, L.; Svane, A.; Szotek, Z.; Temmerman, W. M. First-principles calculations of $\text{PuO}_{2\pm x}$. *Science* **2003**, *301*, 498.
- (27) Sanchez, A. L. Chemical Speciation and Adsorption Behavior of Plutonium in Natural Waters, in Oceanography. Dissertation, University of Washington, 1983.
- (28) Righetto, L.; Bidoglio, G.; Azimonti, G.; Bellebono, I. R. Competitive actinide interaction in colloidal humic acid-mineral oxide systems. *Environ. Sci. Technol.* **1991**, *25*, 1913.
- (29) Runde, W.; Conradson, S. D.; Efurud, D. W.; Lu, N. P.; VanPelt, C. E.; Tait, C. D. Solubility and sorption of redox-sensitive radionuclides (Np, Pu) in J-13 water from the Yucca Mountain site: Comparison between experiment and theory. *Appl. Geochem.* **2002**, *17*, 837.
- (30) Powell, B. A.; Kersting, A. B.; Zavarin, M. In *Hydrologic Resources Management Program and Underground Test Area Project*; FY 2006 Progress Report, LLNL-TR-404620; Zavarin, M., Kersting, A. B., Lindvall, R. E., Rose, T. P., Eds.; Lawrence Livermore National Laboratory, U.S. Department of Energy: Livermore, CA, 2008.